INL/CON-22-69306-Revision-0

An Adaptive Geometry-Free Thermo-Mechanical Model for Directed Energy Deposition Process Modeling

September 2022

Changing the World's Energy Future

Dewen Yushu

Idaho National Laboratory

INL/CON-22-69306-Revision-0

An Adaptive Geometry-Free Thermo-Mechanical Model for Directed Energy Deposition Process Modeling

Dewen Yushu

September 2022

Idaho National Laboratory
Idaho Falls, Idaho 83415

http://www.inl.gov

Prepared for the
U.S. Department of Energy
Under DOE Idaho Operations Office
Contract DE-AC07-05ID14517

September 21, 2022

Dewen Yushu

An Adaptive Geometry-Free Thermo-Mechanical Model for Directed Energy Deposition Process Modeling

Idaho National Laboratory

Background & Outline

❑ Background

- Additive manufacturing & Directed Energy Deposition (DED) challenges
- Computational tools show promise for advancing the DED process
- Accurate & efficient computational model is required

❑ Outline

- Material deposition model with mesh adaptivity
- Thermo-mechanical model
- Numerical examples & validation
- Recent advancements

❖ Find the ideal materials

- discover metamaterial
- printability assessment

➢ Challenges of DED (images are from *siemens.com* and *simplfy3d.com)*

❖ Qualify the process

- monitor and avoid print failures
- automate production

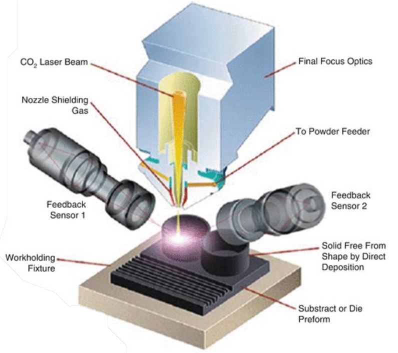

❖ Create a perfect design

- optimize part designs
- optimize printing parameters

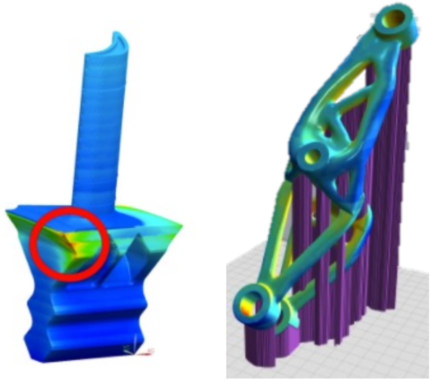

Material Deposition Model

❑ Model material deposition based on subdomain construction

- Decompose the physical domain:

$$\Omega = \Omega_s \cup \Omega_p, \quad \Omega_s \cap \Omega_p = \emptyset$$

- Decompose the product subdomain:

$$\Omega_p = \Omega_a \cup \Omega_i, \quad \Omega_a \cap \Omega_i = \emptyset, \quad \Gamma_{a,i} = \partial\Omega_a \cap \partial\Omega_i$$

- Move elements from inactive subdomain to the active subdomain:

$$\Omega_i \leftarrow \Omega_i \backslash \{\mathcal{T}^\iota\} \quad \text{and} \quad \Omega_a \leftarrow \Omega_a \cup \{\mathcal{T}^\iota\}$$

Ω - Physical domain
Ω_s - Substrate subdomain
Ω_p - Product subdomain
Ω_a - Active product subdomain
Ω_i - Inactive product subdomain
$\Gamma_{a,i}$ - Common interface
$\mathcal{T}^\iota$ - Element in product subdomain

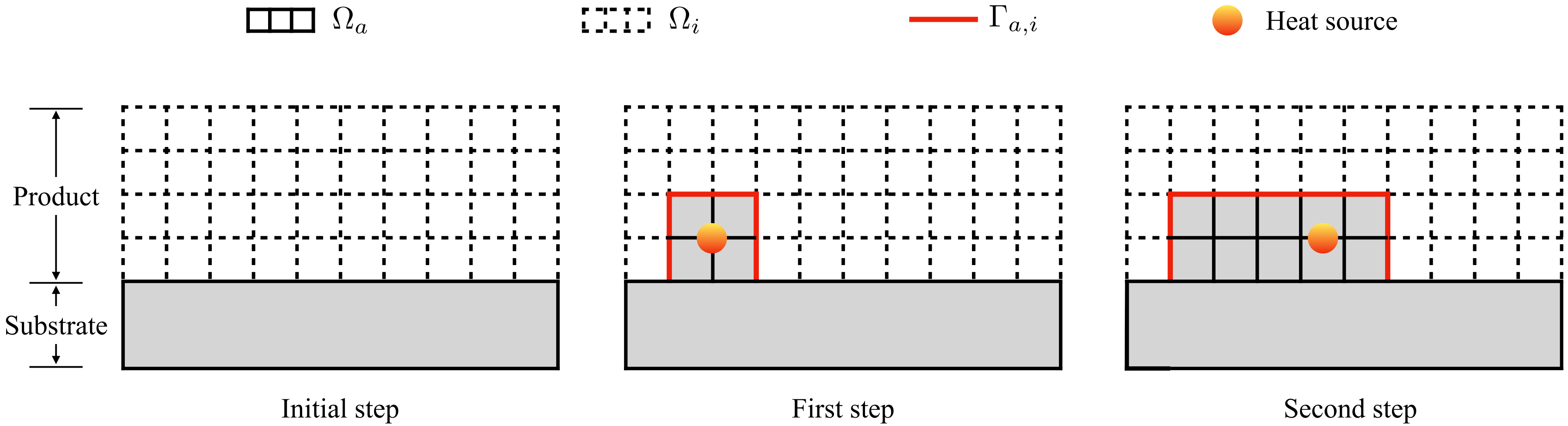

➢ Element activation based on moving subdomains.

Material Deposition Model

❑ Element activation implementation

- Properties and initial conditions are applied to the newly activate elements
- Interface $\Gamma_{a,i}$ is updated
- Boundary conditions (if any) are applied on the updated interface
- Based on block-restricted system in MOOSE

MOOSE

Multiphysics Object-Oriented Simulation Environment

❑ Advantages

- Different definition of MOOSE-based objects in different subdomains
- Only part of the DoFs appear in the system of equations for a typical physics analysis
- Element activation & de-activation
- Open-source to all interested users

Algorithm 1: Element activation: $(\Omega_a, \Omega_i, \Gamma_{a,i}) \leftarrow EA(\Omega_a, \Omega_i, \Gamma_{a,i}, \theta)$

Initialization: activated element set $\mathcal{A} = \emptyset$;
for *each element* $\mathcal{T}^\iota \in \Omega_i$ **do**
  Compute average temperature in $\mathcal{T}^\iota$: $\bar{\theta}^\iota = \left(\int_{\mathcal{T}^\iota} \theta \, \mathrm{d}\Omega\right) / \left(\int_{\mathcal{T}^\iota} 1 \, \mathrm{d}\Omega\right)$;
  if $\bar{\theta}^\iota > \theta_{melt}$ **then**
    Add element to the active element set $\mathcal{A} = \mathcal{A} \cup \{\mathcal{T}^\iota\}$;
    If mesh adaptivity is utilized, move ancestors of $\mathcal{T}^\iota$ to the active subdomain;
if $\mathcal{A} \neq \emptyset$ **then**
  Update subdomains: $\Omega_a = \Omega_a \cup \mathcal{A}$, $\Omega_i = \Omega_i \backslash \mathcal{A}$;
  Update interface and boundary information on $\Gamma = \partial\Omega_a \cap \partial\Omega_i$, $\partial\Gamma_a$, and $\partial\Gamma_i$;
  Project boundary conditions, initial conditions, and material properties in all $\mathcal{T}^\iota \in \mathcal{A}$;

➢ Key steps of the element activation process

Mesh Adaptivity

❑ Subdomain-consistent mesh adaptivity

- Based on existing AMR in MOOSE and LibMesh
- Change parent element subdomain ID during refinement
- Only coarsen an element predicted error is above threshld & all siblings are in the same subdomain

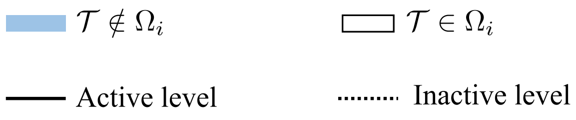

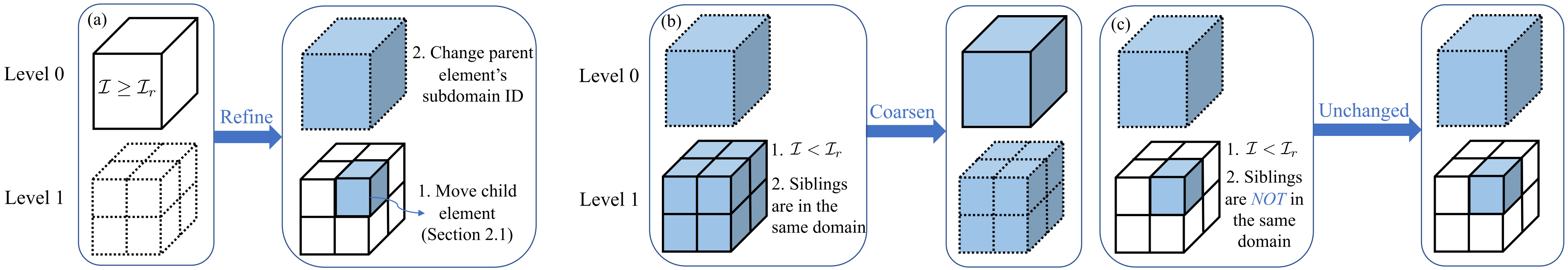

➢ Schematic of the subdomain-consistent mesh adaptivity design. Only two refinement level is shown as an illustration.

❖ **Highly resolved material interface representation**

❖ **Computationally efficient**

Material Deposition Demonstration

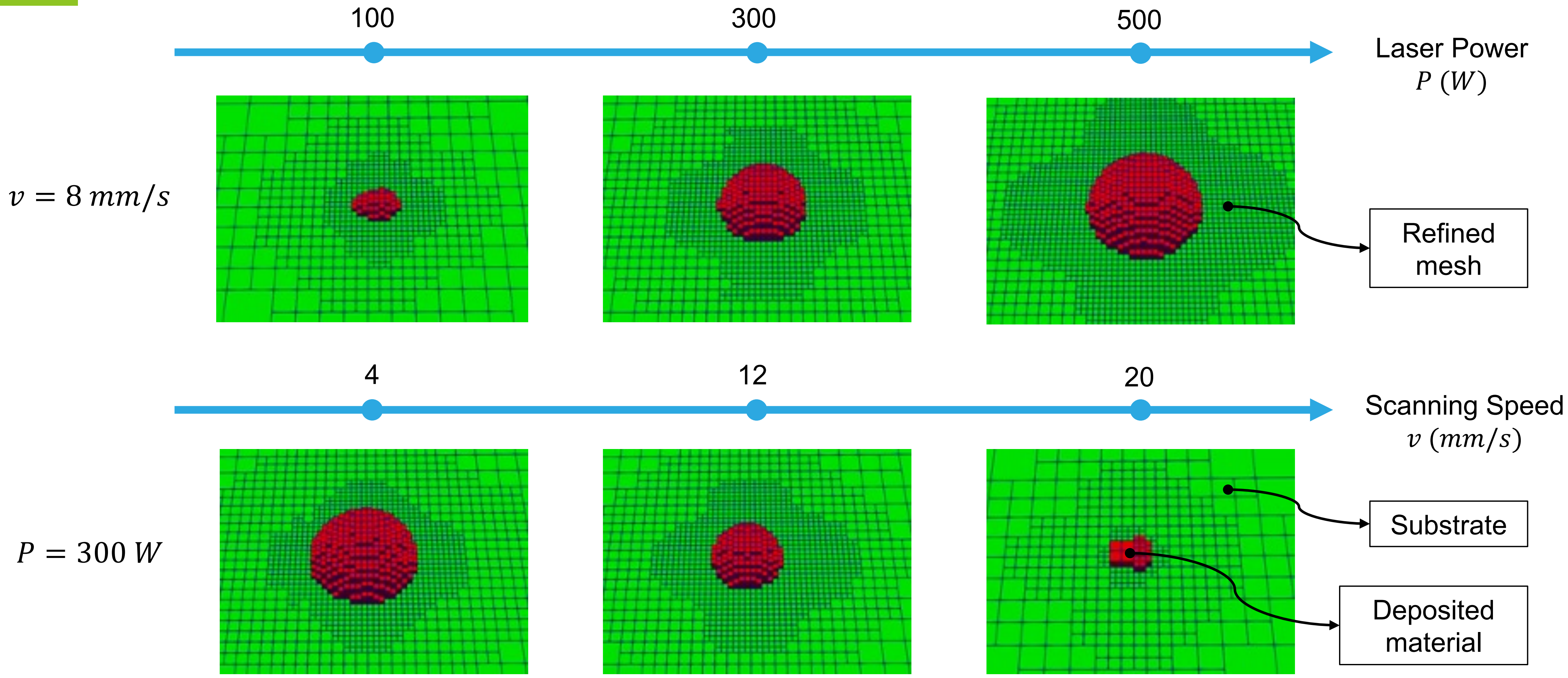

Thermo-mechanical Model – Finite Element Workflow

❑ Main steps

1. Solve the thermal governing equations in the entire domain
2. Mesh adaptivity is conducted based on the predicted temperature field error
3. Move elements that have averaged $\theta > \theta_{melt}$ to the active product subdomain
4. Mechanical deformation due to thermal expansion is analyzed in the substrate and active product subdomain

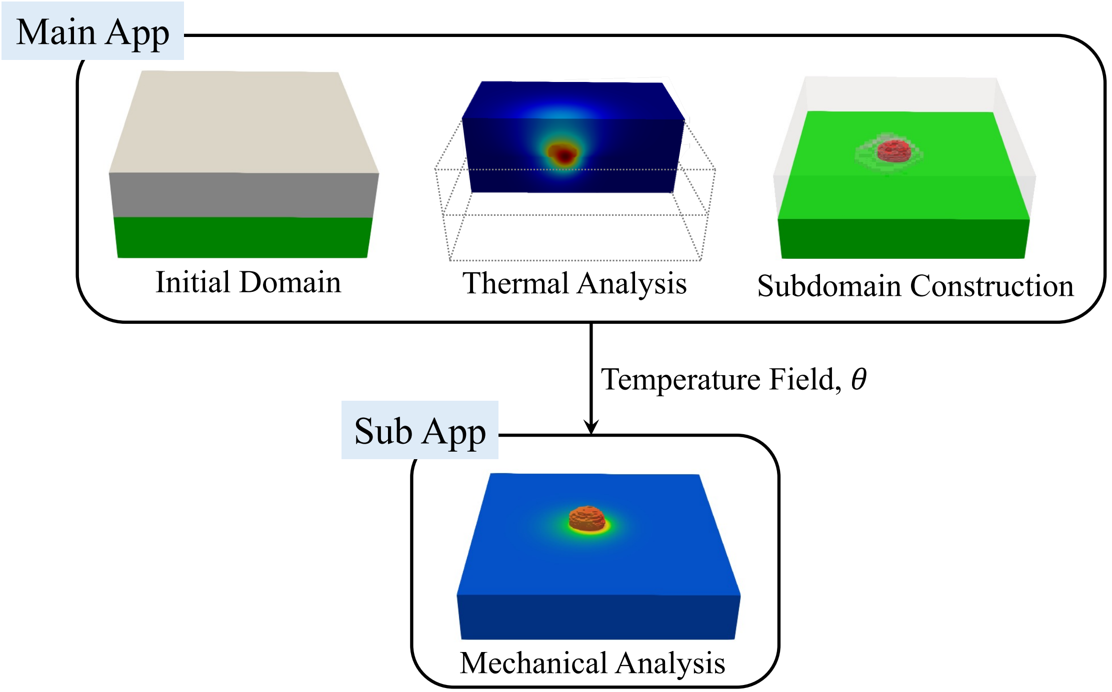

❑ Implementation details

- Multi-app capability
  - Main-app: thermal analysis, mesh adaptivity, material deposition
  - Sub-app: mechanical analysis
- Transfer capability
  - Communicate temperature field from main-app to sub-app
  - Mesh is kept identical between two apps

Thermo-mechanical Model – Thermal Model

Thermal model

- Conservation of energy with a moving heat source and a convective boundary

$$\rho c(\theta)\frac{\partial\theta}{\partial t} = \nabla\cdot\kappa(\theta)\nabla\theta + Q(\boldsymbol{x},t) \quad \text{in } \Omega,$$
$$\theta = \bar{\theta} \quad \text{on } \partial\Omega_{s,\text{bot}},$$
$$-\kappa(\theta)\nabla\theta\cdot\boldsymbol{n} = h(\theta)\cdot(\theta-\bar{\theta}_\infty) \quad \text{on } \Gamma_{a,i}.$$

Moving heat source

- Point heat source:

$$\hat{Q}(\boldsymbol{x},t) = \frac{2\alpha\eta P}{\pi r^3}\exp\left\{-\frac{2||\boldsymbol{x}-\boldsymbol{p}(t)||^2}{r^2}\right\}$$

- Line heat source:

$$\bar{Q}(\boldsymbol{x},t) = \frac{1}{\Delta t}\int_{t_0}^{t_0+\Delta t}\hat{Q}(\boldsymbol{x},t)\ \mathrm{d}t$$

- Hybrid heat source:

$$Q(\boldsymbol{x},t) = \begin{cases}\hat{Q}(\boldsymbol{x},t) & \text{if } \Delta l < L\\ \bar{Q}(\boldsymbol{x},t) & \text{if } \Delta l \geq L\end{cases}$$

θ - Temperature
ρ - Density
$c(\theta)$ - Specific heat (θ dependent)
$\kappa(\theta)$ - Thermal conductivity (θ dependent)
$h(\theta)$ - Heat convection coefficient (θ dependent)
$\bar{\theta}$ - Room temperature
$\bar{\theta}_\infty$ - Temperature far from the boundary
P - Laser power
α - Scaling factor
η - Laser efficiency
r - Effective radius of laser beam
$\boldsymbol{p}(t)$ - Center of laser beam (scanning path)
L - Threshold length
Δl - Laser beam moving distance during one time step

Thermo-mechanical Model – Heat Source Demonstration

❑ Heat source comparison

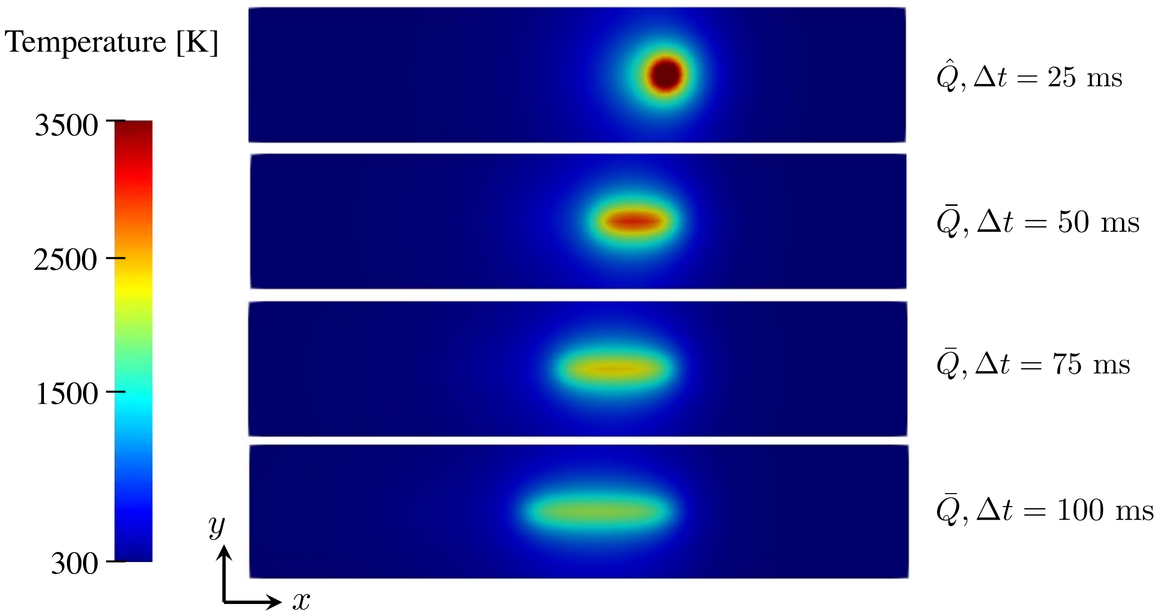

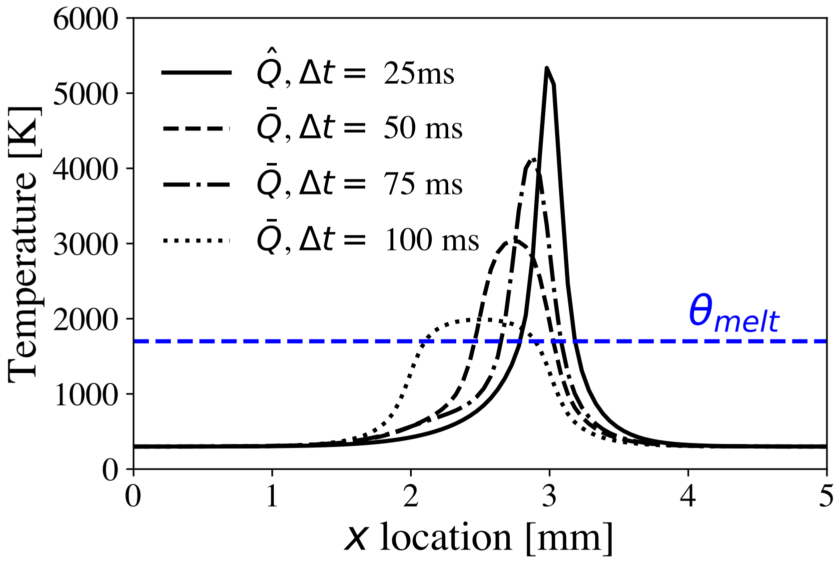

- ➢ Temperature fields of the Gaussian point and line heat sources with different time step sizes.
- ➢ Temperature profile as a function of the x location for the Gaussian point and line heat sources with different time step sizes.

❖ **Hybrid heat source allows for a larger time step size than the point heat source**

❖ **Hybrid heat source is more accurate than the line heat source**

Thermo-mechanical Model – Mechanical Model

❑ Mechanical model

- Quasi-static conservation of momentum

$$\nabla \cdot \boldsymbol{\sigma} + \boldsymbol{b} = 0 \quad \text{in } \Omega_{a,s}$$
$$\boldsymbol{u} = \boldsymbol{0} \quad \text{on } \partial\Omega_{s,\text{bot}}$$

- Power-law hardening elastic-plastic constitutive relation

$$\boldsymbol{\sigma} = \begin{cases} E(\theta)\boldsymbol{\varepsilon}, \boldsymbol{\sigma} \le \boldsymbol{\sigma}_y \\ K\boldsymbol{\varepsilon}^n, \boldsymbol{\sigma} > \boldsymbol{\sigma}_y \end{cases}, \quad \boldsymbol{\sigma}_y = \left(\frac{E^n(\theta)}{K}\right)^{1/(n-1)}$$

- Additively decompose the total strain

$$\boldsymbol{\varepsilon} = \boldsymbol{\varepsilon}_e + \boldsymbol{\varepsilon}_p + \boldsymbol{\varepsilon}_\theta$$

- Strain due to thermal expansion

$$\boldsymbol{\varepsilon}_\theta = \beta(\theta - \theta_0)\boldsymbol{I}$$

$$\theta_0 = \begin{cases} \bar{\theta}_\infty \quad \text{in} \quad \Omega_s \\ \theta_{\text{melt}} \quad \text{in} \quad \Omega_a \end{cases}$$

$\boldsymbol{\sigma}$ - Rank-two Cauchy stress tensor

$\boldsymbol{b}$ - Body force

$\boldsymbol{u}$ - Displacement

$E(\theta)$ - Young's modulus (θ dependent)

K - Strength coefficient

n - Strain hardening coefficient

$\boldsymbol{\sigma}_y$ - Yield stress

$\boldsymbol{\varepsilon}$ - Total strain

$\boldsymbol{\varepsilon}_e, \boldsymbol{\varepsilon}_p, \boldsymbol{\varepsilon}_\theta$ - Elastic, plastic, and thermal strain

β - Thermal expansion coefficient

θ_0 - Stress-free temperature

θ_{melt} - Melt temperature

$\boldsymbol{I}$ - Rank-two identity tensor

Single Track Example

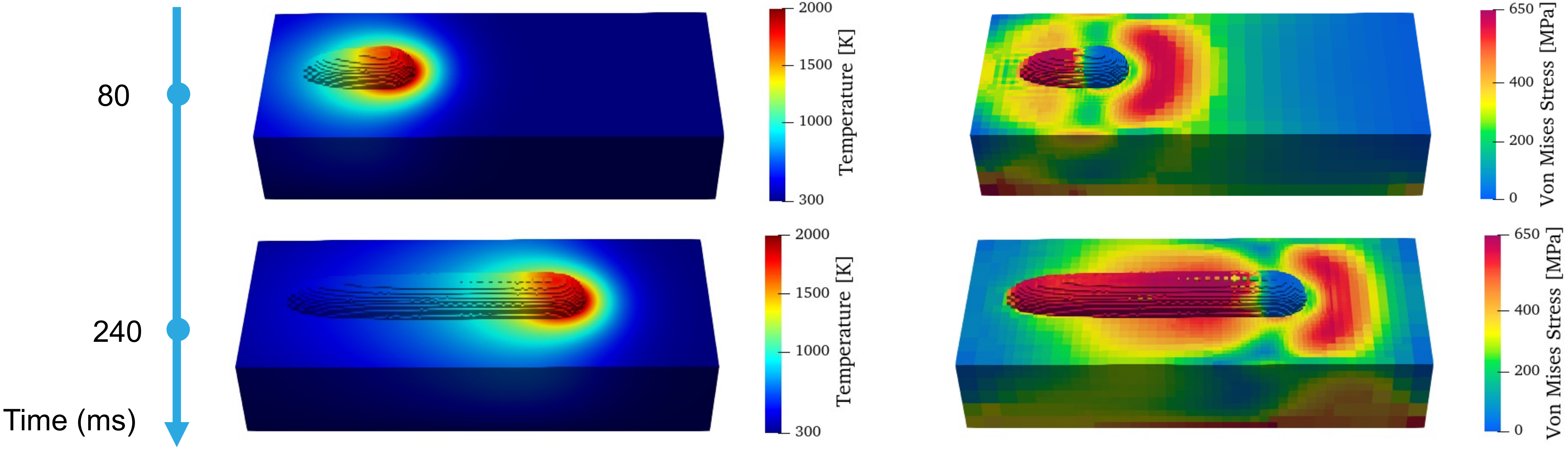

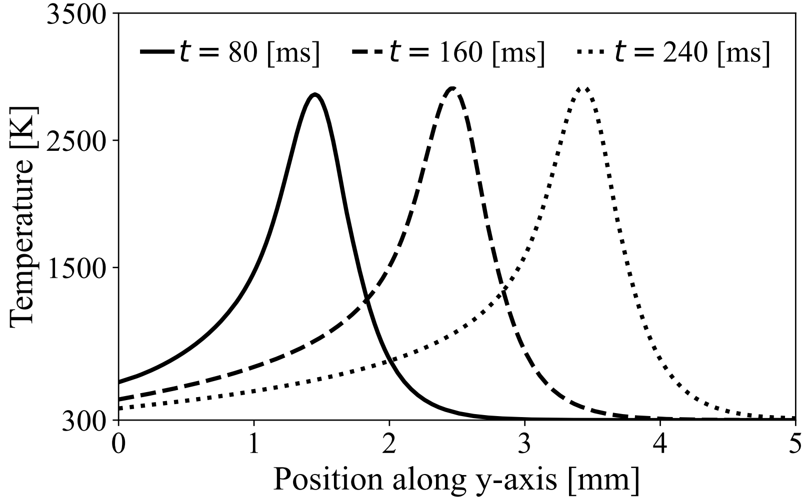

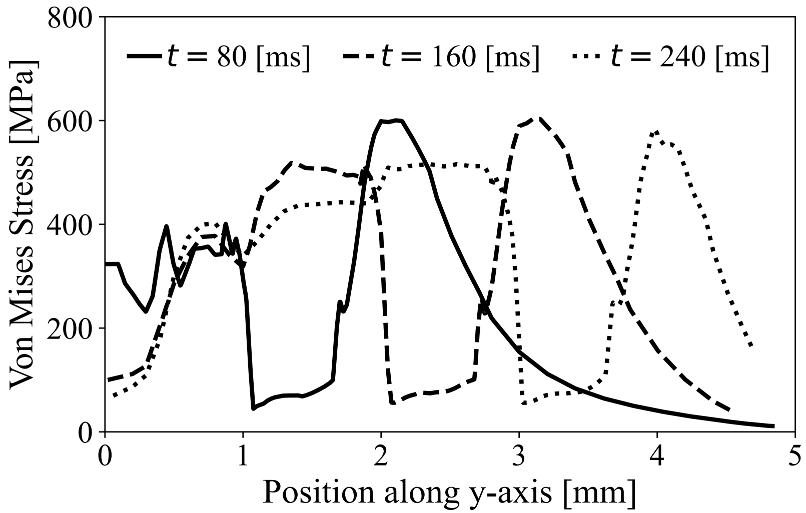

Single Track Example - Validation

❑ Problem setting

- Single track, single layer, scan from 0.5mm – 3.5mm
- 4 laser powers, 4 scanning speeds
- Idaho National Laboratory's Optomec MTS500 LENS DED-type laser/blown- powder 3D metal printer system

Laser Power (W)	Effective Radius (mm)	Scanning Speed (mm/s)
250	0.27	4.23, 6.35, 8.47, 10.58
300	0.30	6.35, 8.47, 10.58, 12.70
350	0.33	8.47, 10.58, 12.70, 14.81
400	0.37	10.58, 12.70, 14.81, 16.93

➢ Simulation parameters for each case

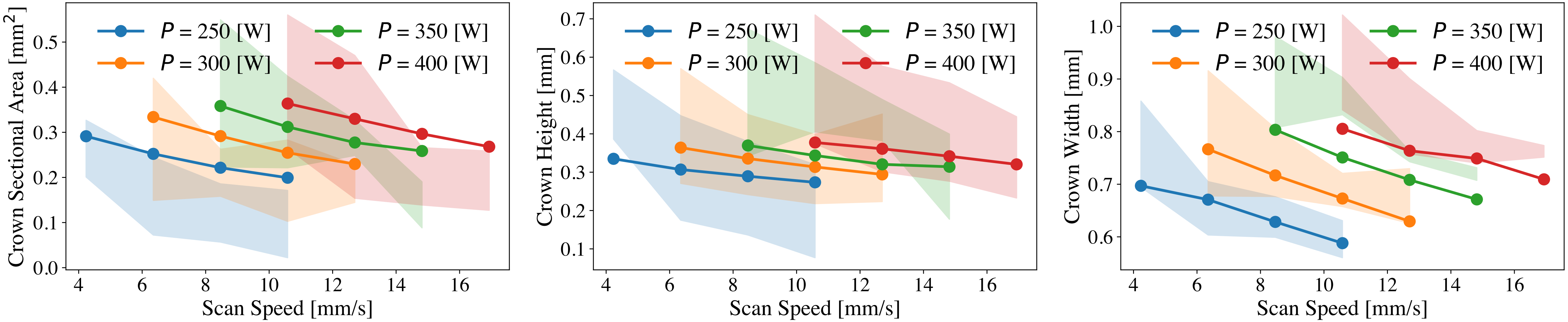

➢ Comparison of simulated and experimental material bead feature sizes

Hollow Cylinder Example

❑ Problem setting

- Domain size $10\ mm \times 10\ mm \times 6\ mm$, initial mesh size $0.25\ mm$
- Scanning path radius $R\ =\ 1.5\ mm$, vertical spacing $l_z = 0.3\ mm$
- Laser power $250\ W$, scanning speed $11.43\ mm/s$

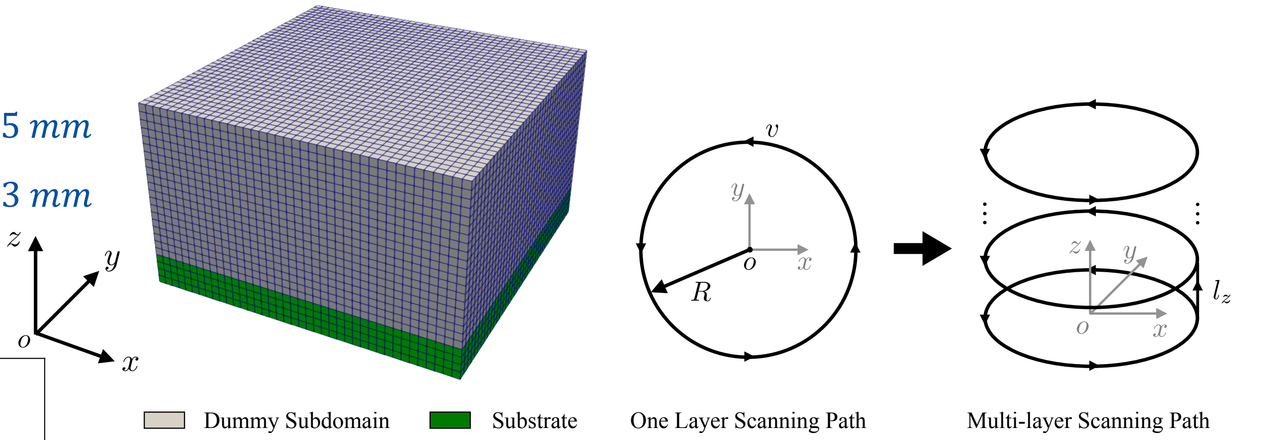

➢ Problem setting for simulating the process of printing a hollow cylinder

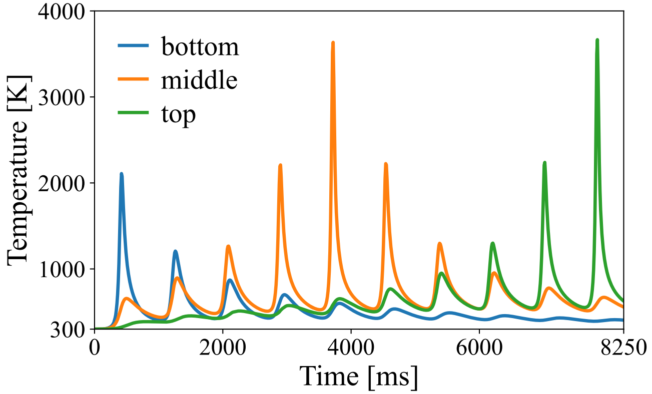

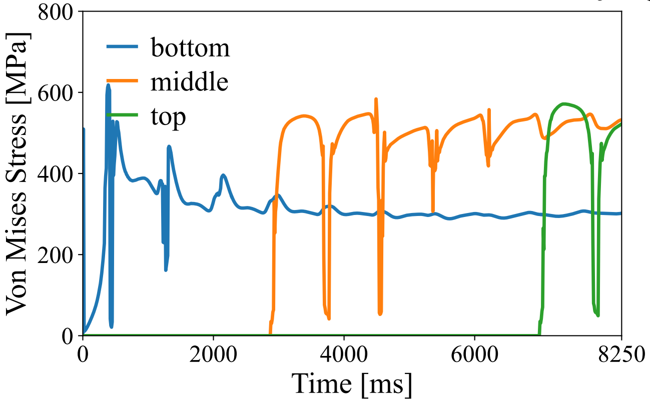

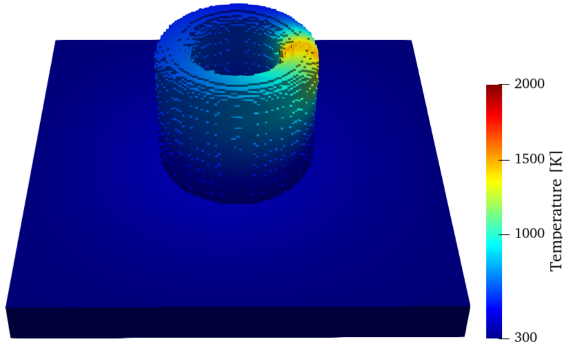

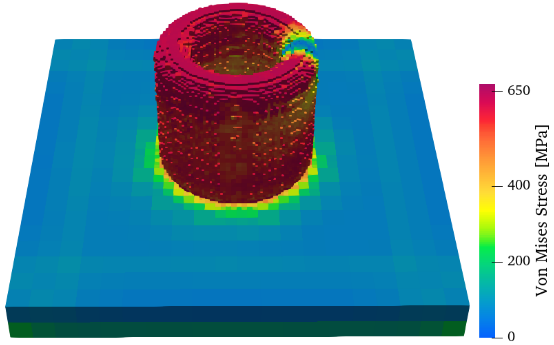

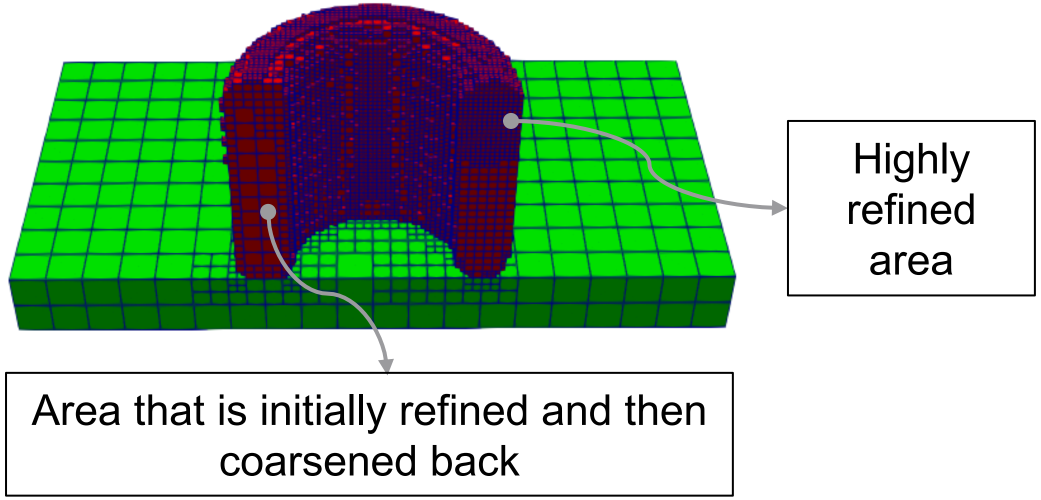

Recent Advancements – Heat Source Improvement

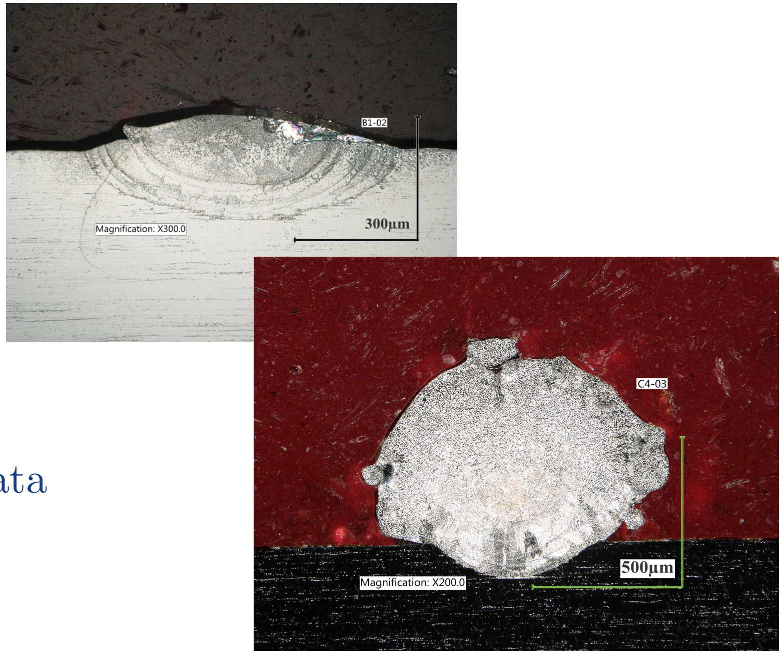

- **Effects from the change of feed-rate**
  - Anisotropic point heat source:

$$\hat{Q}(x,y,z,t) = \frac{2\alpha\eta P}{\pi r_x r_y r_z} \exp\left\{-2\left(\frac{x-p_x(t)}{r_x^2}\right)^2 - 2\left(\frac{y-p_y(t)}{r_y^2}\right)^2 - 2\left(\frac{z-p_z(t)}{r_x^2}\right)^2\right\}$$

  - Effective radii follows normal distributions :

$$r_x, r_y \sim \mathcal{N}\left(\mu_1, \sigma_1^2\right); \quad r_z \sim \mathcal{N}\left(\mu_2, \sigma_2^2\right) \quad \mu_1, \mu_2, \sigma_1, \sigma_2 \text{ are fitted from experimental data}$$

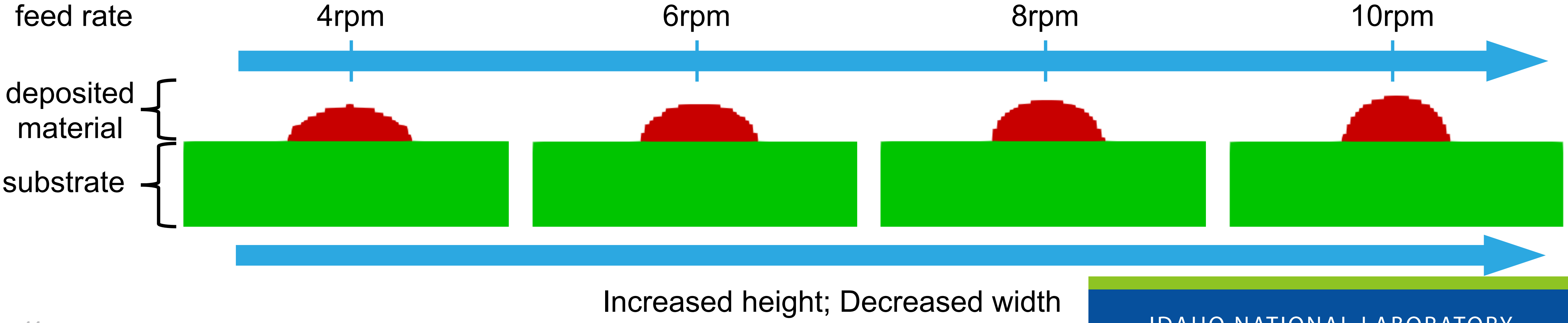

Recent Advancements – Automatic Height Tracking

- **In-situ adjustment of heat source height $p_z(t)$**
  - Capture overbuild during manufacturing
  - Capture overbuild accumulation for higher buildups
  - Heat source height $p_z(t)$ is not an input parameter, but the maximum z-coordinate of the built material in the $(p_x(t), p_y(t))$ plane

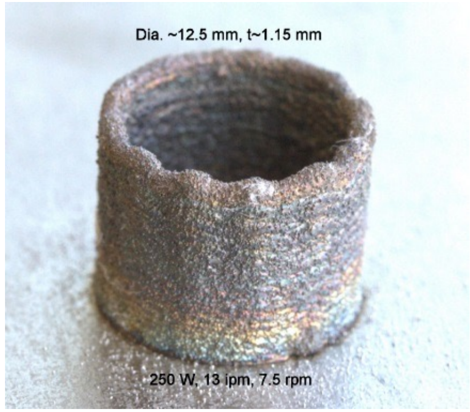

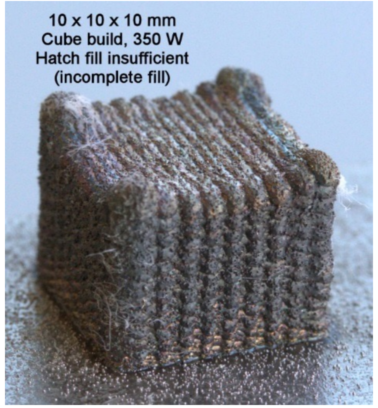

➢ Sub-optimal built parts (over-build along the circumference and at the corners)

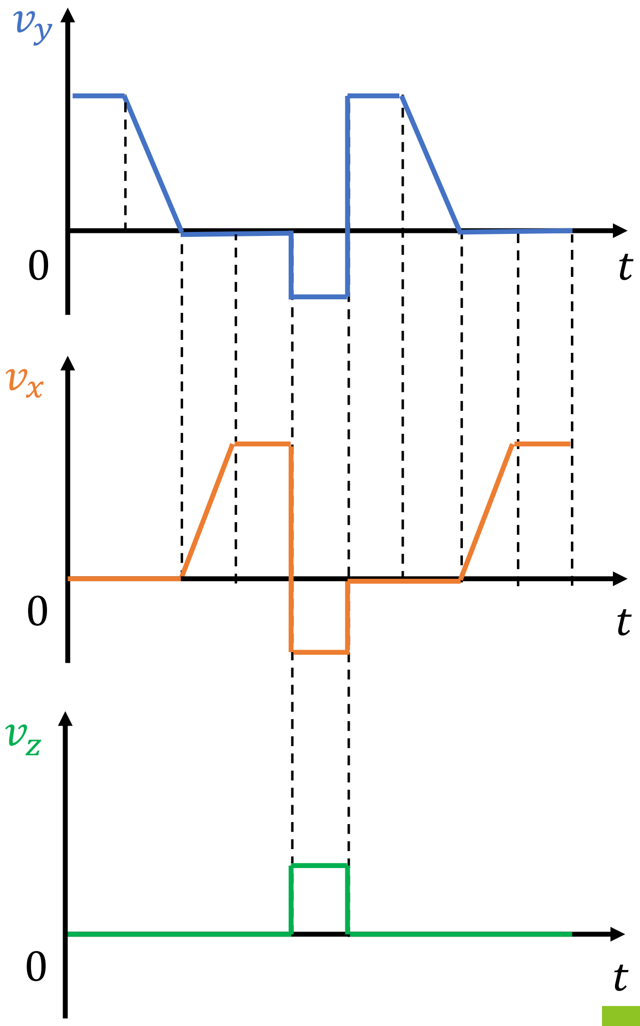

➢ Scanning speed profile

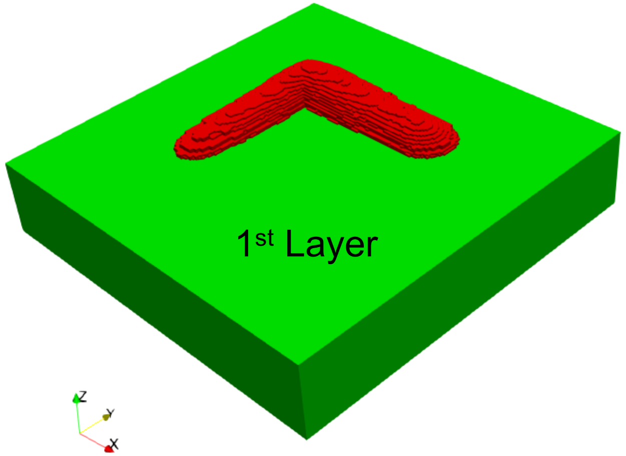

Over-build at the corner

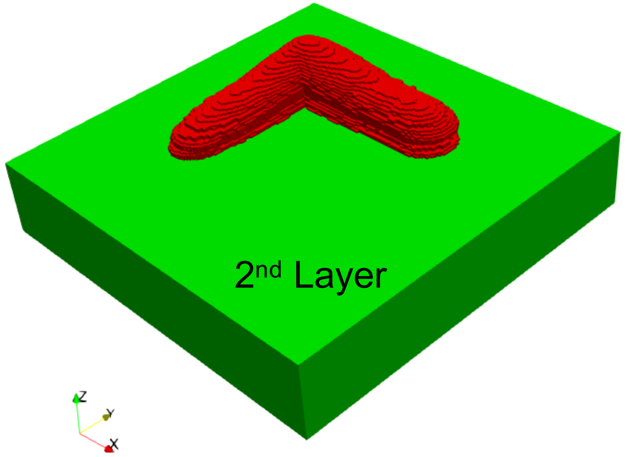

Accumulated over-build

Recent Advancements – Control and Optimization

❑ AI-based process control and optimization

- Develop the neural-network based machine learning capabilities in MOOSE (integration of MOOSE & PyTorch)
- Develop the deep reinforcement learning (DRL)-based control scheme
- Research into DRL algorithms, control workflow

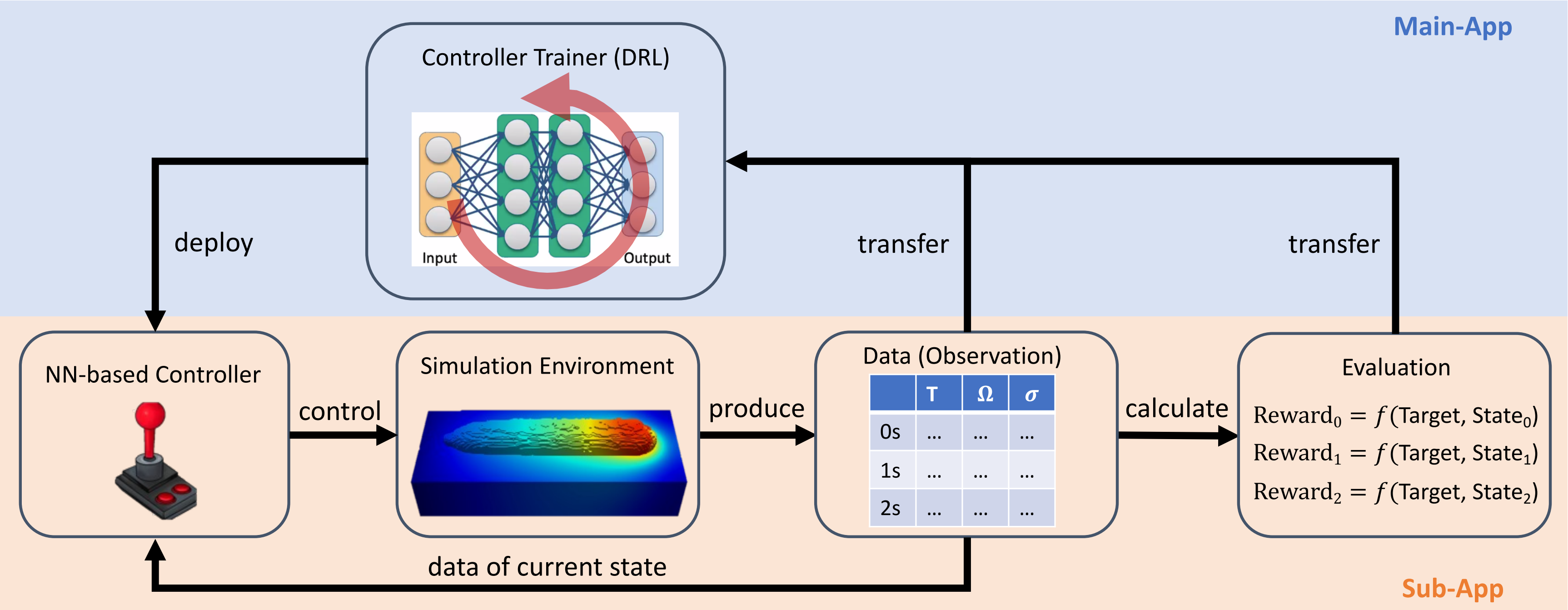

➢ Schematic of the AI-based process control and optimization implementation

References

- Yushu D, McMurtrey MD, Jiang W, Kong F. Directed energy deposition process modeling: A geometry-free thermo-mechanical model with adaptive subdomain construction. The International Journal of Advanced Manufacturing Technology. 2022 Sep;122(2):849-68.
- Grilli N, Hu D, Yushu D, Chen F, Yan W. Crystal plasticity model of residual stress in additive manufacturing using the element elimination and reactivation method. Computational Mechanics. 2022 Mar;69(3):825-45.
- German P, Yushu D. Enabling scientific machine learning in MOOSE using Libtorch. SoftwareX, Submitted, 2022.

Idaho National Laboratory